

A metaproteomic analysis of the response of a freshwater microbial community under nutrient enrichment

David Russo¹, Andrew Beckerman¹, Narciso Couto¹, Jags Pandhal^{1*}

¹University of Sheffield, United Kingdom

Submitted to Journal:
Frontiers in Microbiology

Specialty Section:
Aquatic Microbiology

ISSN:
1664-302X

Article type:
Original Research Article

Received on:
27 Jan 2016

Accepted on:
14 Jul 2016

Provisional PDF published on:
14 Jul 2016

Frontiers website link:
www.frontiersin.org

Citation:

Russo D, Beckerman A, Couto N and Pandhal J(2016) A metaproteomic analysis of the response of a freshwater microbial community under nutrient enrichment. *Front. Microbiol.* 7:1172. doi:10.3389/fmicb.2016.01172

Copyright statement:

© 2016 Russo, Beckerman, Couto and Pandhal. This is an open-access article distributed under the terms of the [Creative Commons Attribution License \(CC BY\)](http://creativecommons.org/licenses/by/4.0/). The use, distribution and reproduction in other forums is permitted, provided the original author(s) or licensor are credited and that the original publication in this journal is cited, in accordance with accepted academic practice. No use, distribution or reproduction is permitted which does not comply with these terms.

This Provisional PDF corresponds to the article as it appeared upon acceptance, after peer-review. Fully formatted PDF and full text (HTML) versions will be made available soon.

1 **A metaproteomic analysis of the response of a freshwater**
2 **microbial community under nutrient enrichment**

3
4 **David A. Russo¹, Narciso Couto¹, Andrew Beckerman², Jagroop Pandhal^{1*}**

5 ^aDepartment of Chemical and Biological Engineering, University of Sheffield, Mappin Street,
6 Sheffield S1 3JD, United Kingdom

7 ^bDepartment of Animal and Plant Sciences, University of Sheffield, Alfred Denny Building,
8 Western Bank, Sheffield, S10 2TN, UK

9
10 *Correspondence: Jagroop Pandhal, Department of Chemical and Biological Engineering,
11 University of Sheffield, Mappin Street, Sheffield S1 3JD, United Kingdom.

12 j.pandhal@sheffield.ac.uk

13
14 **Keywords: oligotrophic, eutrophic, metaproteomics, microbial loop, algae, freshwater**

Provisional

15 **Abstract**

16

17 Eutrophication can lead to an uncontrollable increase in algal biomass, which has
18 repercussions for the entire microbial and pelagic community. Studies have shown how
19 nutrient enrichment affects microbial species succession, however details regarding the
20 impact on community functionality are rare. Here, we applied a metaproteomic approach to
21 investigate the functional changes to algal and bacterial communities, over time, in
22 oligotrophic and eutrophic conditions, in freshwater microcosms. Samples were taken early
23 during algal and cyanobacterial dominance and later under bacterial dominance. 1048
24 proteins, from the two treatments and two timepoints, were identified and quantified by their
25 exponentially modified protein abundance index. In oligotrophic conditions, Bacteroidetes
26 express extracellular hydrolases and Ton-B dependent receptors to degrade and transport high
27 molecular weight compounds captured while attached to the phycosphere. Alpha- and Beta-
28 proteobacteria were found to capture different substrates from algal exudate (carbohydrates
29 and amino acids, respectively) suggesting resource partitioning to avoid direct competition.
30 In eutrophic conditions, environmental adaptation proteins from cyanobacteria suggested
31 better resilience compared to algae in a low carbon nutrient enriched environment. This study
32 provides insight into differences in functional microbial processes between oligo- and
33 eutrophic conditions at different timepoints and highlights how primary producers control
34 bacterial resources in freshwater environments.

Provisional

1. Introduction

Freshwater ecosystems are subjected to nutrient enrichment on a local, regional and global scale in a process known as eutrophication. Due to human activity, global aquatic fluxes of nitrogen and phosphorus have been amplified by 108% and 400%, respectively (Falkowski et al., 2000). These nutrient imbalances have led to a drastic increase in the occurrence of algal blooms, an event where photoautotrophic biomass may increase by several orders of magnitude (Elser et al., 2007). During a bloom, high amounts of organic carbon and nutrients are channeled through the bacterial community and made available for higher trophic levels in what is known as the microbial loop (Azam et al., 1983). The microbial loop plays a crucial role in the biogeochemical cycling of elements, such as carbon, phosphorus and nitrogen, as well as organic matter. It is ultimately responsible for a substantial fraction of aquatic nutrient and energy fluxes (Azam and Malfatti, 2007). Thus, a better understanding of how the microbial loop and associated algae respond to nutrient enrichment, can reveal important features of how ecosystem processes are affected by eutrophication.

The development and application of “omics” technologies has allowed for an unprecedented view of microbial dynamics and their role in driving ecosystem function, including biogeochemical cycling of elements and decomposition and remineralization of organic matter. One approach is to obtain and sequence DNA from the microbial community in order to provide access to the genetic diversity of a microbial community (metagenomics). However, the genetic diversity gives us an incomplete view of what role these genes have in community processes. In contrast, metaproteomics can relate the intrinsic metabolic function by linking proteins to specific microbial activities and to specific organisms. Metaproteomics can thus address the long-standing objective in environmental microbiology of linking the identity of organisms comprising diversity in a community to ecosystem function (Hettich et al., 2013).

In the last few years metaproteomics has had a growing influence in aquatic environmental microbiology. It has been used to address questions about diversity, functional redundancy and provision of ecosystem services including nutrient recycling and energy transfer. For example, in one of the metaproteomic pioneering studies Giovannoni et al. (2005) demonstrated the ubiquity of proteorhodopsin-mediated light-driven proton pumps in bacteria (Giovannoni et al., 2005). Later, a study by Sowell et al. (2011) was the first of its kind to demonstrate the importance of high affinity transporters for substrate acquisition in marine bacteria (Sowell et al., 2011a). Although most of the notable metaproteomic aquatic studies have focused on marine environments, the tool has also been used in freshwater environments to examine, for example, the functional metaproteomes from the meromictic lake ecosystem in Antarctica (Ng et al., 2010; Lauro et al., 2011) or the microbes in Cayuga and Oneida Lake, New York (Hanson et al., 2014). The application of metaproteomics in such studies have successfully provided details regarding the importance of bacteriochlorophyll in the adaptation to low light (Ng et al., 2010), the metabolic traits that aid life in cold oligotrophic environments (Lauro et al., 2011) and nutrient cycling, photosynthesis and electron transport in freshwater lakes (Hanson et al., 2014)

In this paper we report a comprehensive discovery-driven (Aebersold et al., 2000) metaproteomic analysis of a freshwater microbial community under differing nutrient regimes to elucidate the predominant metabolic processes in each conditions. We expect that, overall, bacterial growth and abundance will be higher in the oligotrophic treatment but certain algal-bacterial processes (e.g. metabolite exchange) can benefit the microalgal

85 community. In the eutrophic treatment, where algae have a growth advantage, proteins
86 related to photosynthesis and energy generation should be highly expressed while it is
87 expected that bacteria express proteins that aid adaptation to low dissolved organic matter
88 (DOM) environments (e.g. switch from heterotrophy to autotrophy).

89
90 We inoculated microcosms with a microbial community subjected to two nutrient treatments
91 to mimic oligotrophic and eutrophic conditions in freshwater lakes. Microcosms, as
92 experimental systems, provide evidence for or against hypotheses that are difficult to test in
93 nature (Drake and Kramer, 2011) and, here, allowed us to focus on the effects of nutrient
94 enrichment on the microbial community. Bacterial, cyanobacteria and algal abundances were
95 quantified throughout the experiment as were physicochemical measurements. The microbial
96 metaproteome was extracted from two nutrient treatments (oligotrophic and eutrophic) at two
97 time points. The time points were selected to represent phases of algal/cyanobacterial
98 dominance and, later, heterotrophic bacterial dominance. For each treatment the extracted
99 proteome was analyzed by nano-liquid chromatography–tandem mass spectrometry (LC-
100 MS/MS). A meta-genetic community analysis of prokaryotic and eukaryotic diversity within
101 the inoculum was used to generate a refined protein database for identifying proteins at the
102 specified time-points. This approach reduced the spectral search space and led to reliable
103 false discovery rate statistics (Jagtap et al., 2013). The identified proteins at the two time
104 points were then grouped into taxonomic and functional categories to link identity with
105 function (Pandhal et al., 2008). We analyzed changes in protein expression in individual
106 phylogenetic groups, over time and in both nutrient concentrations, to give an insight into the
107 functional attributes of the major microbial players in the experimental microcosm
108 community.

109 **2. Materials and Methods**

110 **2.1. Microcosm setup**

111
112
113 We constructed replicate experimental biological communities in 30 L white, opaque,
114 polypropylene vessels, 42 cm high and with an internal diameter of 31 cm. The microcosms
115 were housed in controlled environment facilities at the Arthur Willis Environmental Centre at
116 the University of Sheffield, U.K. These were filled with 15 L of oligotrophic artificial
117 freshwater growth medium (for detailed composition see Supp. Mat. Table 1). Over the
118 course of the experiment the microcosms were kept at constant temperature, 23°C, under 100
119 $\mu\text{mol m}^{-2} \text{ s}^{-1}$, provided by Hellelamp 400 watt IR Lamps HPS (Helle International Ltd., UK),
120 and 12:12 light dark cycle. A microbial community was introduced into each microcosm
121 (detailed composition in Supp. Mat. Table 2 and 3). This inoculum was sourced from 100L of
122 water samples collected at Weston Park Lake, Sheffield, U.K. (53°22'56.849'' N,
123 1°29'21.235'' W). The inoculum was filtered with a fine mesh cloth (maximum pore size 200
124 μm) to exclude big particles, protists and grazer populations (Downing, Osenberg & Sarnelle,
125 1999). The filtered sample was cultured for five days in the conditions described to allow
126 acclimation to the controlled conditions. Subsequently, each 15 L media was inoculated with
127 2.5 L of this sample.

128
129 The inoculated microcosms were subjected to two nutrient treatments to mimic oligotrophic
130 and eutrophic conditions in freshwater lakes. Our experimental elevation of initial nutrient
131 levels followed United States Environmental Protection Agency guidelines for oligotrophic
132 and eutrophic conditions in freshwater lakes and reservoirs (USEPA, 1986): (1) non-enriched
133 growth medium to simulate oligotrophic conditions ($\text{NO}_3^- = 0.42 \text{ mg L}^{-1}$ and $\text{PO}_4^{3-} = 0.03$
134 mg L^{-1}) and (2) NO_3^- and PO_4^{3-} enriched growth medium ($\text{NO}_3^- = 4.20 \text{ mg L}^{-1}$ and PO_4^{3-}

135 = 0.31 mg L⁻¹) to simulate eutrophic conditions. Each treatment was replicated eighteen
136 times, allowing for serial but replicated (n=3 biological replicate microcosms) destructive
137 sampling during the experiment. The experiment was run for 18 days to allow the added
138 NO₃⁻ and PO₄³⁻ to deplete and generate batch microbial growth curves (see Fig. 1). We also
139 followed three control microcosms comprised of non-enriched growth medium, with no
140 biological inoculum, allowing us to follow physicochemical variation in the absence of
141 introduced biological activity (see Supp. Mat. Fig. 1).

142
143

144 2.2. Sampling of abiotic variables

145

146 Over the course of the experiment dissolved oxygen (DO), pH, temperature, nitrate (NO₃⁻)
147 and phosphate (PO₄³⁻) were monitored in order to link the abiotic variation to the changes
148 observed in the biological variables. DO, pH and temperature were measured at 12:00 and
149 18:00 daily with a Professional Plus Quatro (YSI, USA). 15 mL aliquots were collected and
150 filtered (0.45 μm), daily, for the estimation of NO₃⁻ and PO₄³⁻ concentrations. NO₃⁻ was
151 estimated with a Dionex ICS-3000 ion chromatograph (Thermo Fisher Scientific, USA) using
152 an AG18 2x250 mm column with a 0.25 mL min⁻¹ flow rate and 31.04 mM potassium
153 hydroxide as eluent. PO₄³⁻ concentrations were measured according to protocols defined by
154 British standards (BS EN ISO 6878:2004) (BSI, 2004).

155

156 2.3. Sampling of biotic variables

157

158 To estimate microalgae and cyanobacterial abundance, fluorescence was measured daily, at
159 12:00, with the AlgaeTorch (bbe Moldaenke GmbH, Germany). By measuring fluorescence,
160 at 470 nm, 525 nm and 610 nm for chlorophyll *a* and phycocyanin, the two spectral groups of
161 microalgae and cyanobacteria, can be differentiated *in situ*. The relative amount of each
162 group, expressed in terms of the equivalent amount of biomass per liter of water, was
163 calculated according to (Beutler et al., 2002).

164

165 Culturable heterotrophic bacteria were enumerated as an estimation of total bacteria (Lehman
166 et al., 2001; Eaton and Franson, 2005; CSLC, 2009; Perkins et al., 2014) every three days by
167 sampling 100 μL aliquots, in triplicate, plating on R2A agar (Oxoid, UK), incubating for 24 h
168 at 37°C and counting colony forming units (CFU per mL). CFU were calculated with
169 OpenCFU software (Geissmann, 2013). Because bacteria were only enumerated every three
170 days, we used linear interpolation to generate a daily time series to obtain a uniform sample
171 size across all variables. Interpolated values were calculated using the formula:

172

$$173 \quad y = y_1 + (y_2 - y_1) \frac{x - x_1}{x_2 - x_1}$$

174

175 where *y* is the missing value, *x* is the missing time point, *y*₁, *y*₂ are the two closest measured
176 bacterial counts and *x*₁, *x*₂ are the respective time points.

177

178 2.4. Protein preparation

179

180 Microcosm samples were concentrated, in triplicate, at days three and 12 of the time course
181 using a Centrimate tangential flow filtration (TFF) system fitted with three 0.1 μm pore size
182 Supor TFF membranes (Pall Corporation, USA). After every use, the filter system was
183 sanitized with a 0.5 M sodium hydroxide solution and flushed with deionized water. The
184 permeate was then filtered with a 3 μm pore size polycarbonate isopore membrane (EMD

185 Millipore, USA) in order to obtain fractions dominated by free-living bacteria (<3 μm in size)
186 and alga and particle-associated bacteria (>3 μm in size) (Teeling et al., 2012). These
187 fractions were harvested at $10\,000 \times g$ for 15 minutes at 4°C . The resulting cell pellets were
188 further washed in 0.5 M triethylammonium bicarbonate buffer (TEAB) prior to storage at -
189 20°C . Cells were defrosted and resuspended in extraction buffer (250 μL of 0.5 M TEAB,
190 0.1% sodium dodecyl sulfate (SDS)) and 1 μL of halt protease inhibitor cocktail (Fisher
191 Scientific, USA)) incorporating a sonication bath step for 5 minutes wiogunth ice. The
192 resulting suspension was submitted to five freeze-thaw cycles (each cycle corresponds to two
193 minutes in liquid nitrogen and five minutes in a 37°C water bath) (Ogunseitan, 1993). The
194 lysed sample was centrifuged at $15,000 \times g$ for 10 minutes at 4°C and the supernatant was
195 transferred to a LoBind microcentrifuge tube (Eppendorf, Germany). The remaining cell
196 pellet was resuspended in extraction buffer (125 μL) and homogenized with glass beads (425-
197 600 μm) for ten cycles (each cycle corresponds to two minutes homogenization and two
198 minutes on ice). The lysed sample was centrifuged at $15,000 \times g$ for 10 minutes at 4°C and
199 the supernatants from both extraction methods were combined. 1 μL of benzonase nuclease
200 (Sigma-Aldrich, USA) was added to the collected supernatants. Extracted proteins were
201 precipitated overnight, at -20°C , using four volumes of acetone. The dried protein pellet was
202 resuspended in 100 μL of 0.5 M TEAB and quantified using the 230/260 spectrophotometric
203 assay described by Kalb and Bernlohr (Kalb and Bernlohr, 1977). Biological replicates were
204 pooled before reduction, alkylation and digestion. This approach has been shown to be
205 potentially valuable for proteomics studies where low amount of protein does not allow
206 replication (Diz et al., 2009) whilst enhancing the opportunity to identify lower abundance
207 proteins. Moreover, the small variances observed between replicate microcosms in terms of
208 all biological and physiochemical measurements conducted (Fig. 1, Supp. Mat. Fig. 1) gave
209 further confidence to this approach. Protein samples (200 μg) were reduced with 20 mM tris-
210 (2-carboxyethyl)-phosphine, at 60°C for 30 min, followed by alkylation with 10 mM
211 iodoacetamide for 30 minutes in the dark. Samples were digested overnight, at 37°C , using
212 trypsin (Promega, UK) 1:40 (trypsin to protein ratio) resuspended in 1 mM HCl. The samples
213 were dried using a vacuum concentrator and stored at -20°C prior to fractionation.

214 215 **2.5. Chromatography and mass spectrometry**

216
217 The first dimensional chromatographic separation, off-line, was performed on a Hypercarb
218 porous graphitic column (particle size: 3 μm , length: 50 mm, diameter: 2.1 mm, pore size: 5
219 μm) (Thermo-Dionex, USA) on an Ultimate 3000 UHPLC (Thermo-Dionex, USA). Peptides
220 were resuspended in 200 μL of Buffer A (0.1% (v/v) trifluoroacetic acid (TFA) and 3% (v/v)
221 HPLC-grade acetonitrile (ACN) in HPLC-grade water) and eluted using a linear gradient of
222 Buffer B (0.1% (v/v) TFA and 97% (v/v) ACN in HPLC-grade water) ranging from 5 to 60%
223 over 120 minutes with a flow rate of 0.2 mL min^{-1} . Peptide elution was monitored at a
224 wavelength of 214 nm and with Chromeleon software, version 6.8 (Thermo-Dionex, USA).
225 Fractions were collected every two minutes, between 10 and 120 minutes, using a Foxy
226 Junior (Teledyne Isco, USA) fraction collector and dried using a vacuum concentrator. Dried
227 fractions were stored at -20°C prior to mass spectrometry analysis. The second dimensional
228 chromatographic separation of each peptide fraction was performed on a nano-LC-ESI-
229 MS/MS system. In this system a U3000 RSLCnano LC (Thermo-Dionex, USA), containing a
230 trap column (300 $\mu\text{m} \times 5\text{ mm}$ packed with PepMap C18, 5 μm , 100 \AA wide pore, Dionex)
231 followed by a reverse phase nano-column (75 $\mu\text{m} \times 150\text{ mm}$ packed with PepMap C18, 2
232 μm , 100 \AA wide pore, Dionex), was coupled to an ultra-high resolution quadrupole time-of-
233 flight (UHR maXis Q-ToF 3G) mass spectrometer (Bruker, Germany) equipped with an
234 Advance CaptiveSpray ion source. Peptide fractions were resuspended in loading buffer

235 (0.1% (v/v) TFA and 3% (v/v) ACN in HPLC-grade water) and two injections were made. A
236 90 minute linear gradient elution was performed using buffer A (0.1% (v/v) formic acid (FA)
237 and 3% (v/v) ACN in HPLC-grade water) and buffer B (0.1% (v/v) FA and 97% (v/v) ACN
238 in HPLC-grade water), during which buffer B increased from 4 to 40% at a flow rate of 0.3
239 $\mu\text{L min}^{-1}$. On the mass spectrometer, the following settings were specified: endplate Offset -
240 500 V, capillary voltage 1000 V, nebulizer gas 0.4 bar, dry gas 6.0 L min^{-1} , and dry
241 temperature 150 °C. Mass range: 50-2200 m/z , at 4 Hz. Lock mass was used for enabling
242 mass acquisition correction in real time, therefore high mass accuracy data were obtained.
243 Data were acquired for positive ions in a dependent acquisition mode with the three most
244 intense double, triple or quadruple charges species selected for further analysis by tandem
245 mass spectrometry (MS/MS) under collision induced dissociation (CID) conditions where
246 nitrogen was used as collision gas.

247

248 **2.6. 16S and 18S rDNA gene sequencing of inoculum**

249

250 **2.6.1. DNA extraction**

251

252 Inoculum samples were lysed in 50 mM Tris-HCl (pH 8.0), 10 mM EDTA and 10% (w/v)
253 SDS by vortexing with glass beads. DNA was extracted with a standard phenol-chloroform
254 extraction protocol (Sambrook and Russel, 2001). The DNA was precipitated using sodium
255 acetate (50 μL of 3 M stock solution, pH 4.8-5.2) and ice-cold ethanol. PCR amplification,
256 product pooling, purification sequencing and bioinformatics and statistical analysis were
257 performed by Research and Testing Laboratory (Texas, USA).

258

259 **2.6.2. PCR amplification**

260

261 Markers were amplified from DNA extractions using adapted Illumina tagged primers.
262 Forward primers were constructed with Illumina adapter i5
263 (AATGATACGGCGACCACCGAGATCTACAC) an 8-10bp barcode, a primer pad and
264 either primer 28F (GAGTTTGATCNTGGCTCAG) or TAREukF
265 (CCAGCASCYGCGGTAATTCC). Reverse primers were constructed with Illumina adapter
266 i7 (CAAGCAGAAGACGGCATAACGAGAT) an 8-10bp barcode, a primer pad and either
267 primer 519R (GTNTTACNGCGGCKGCTG) or TAREukR (ACTTTCGTTCTTGATYRA).
268 Primer pads were used to ensure a primer melting temperature of 63°C-66°C, as per the
269 Schloss method (Schloss et al., 2009). Reactions were performed using corresponding primer
270 pairs (i.e. 28F x 519R and TAREukF x TAREukR) using the Qiagen HotStar Taq master mix
271 (Qiagen Inc, Valencia, California) adding 1 μL of each 5 μM primer, and 1 μL of template to
272 make a final 25 μL reaction volume, with a thermal cycling profile of 95°C for 5 min., then
273 35 cycles of 94°C for 30 sec., 54°C for 40 sec., 72°C for 1 min., followed by one cycle of
274 72°C for 10 min. Amplified products were visualized with eGels (Life Technologies, Grand
275 Island, New York) and pooled. Pools were purified (size selected) through two rounds of 0.7x
276 Agencourt AMPure XP (BeckmanCoulter, Indianapolis, Indiana) as per manufacturer's
277 instructions, before quantification with a Qubit 2.0 fluorometer (Life Technologies). Finally
278 pools were loaded and sequenced on an Illumina MiSeq (Illumina, Inc. San Diego,
279 California) 2x300 flow cell at 10 pM. The sequence data are available from the European
280 Nucleotide Archive under Study Accession Number PRJEB12443, and Sample Accession
281 Numbers ERS1037123 (16S DNA) and ERS1037124 (18S DNA).

282

283 **2.6.3. Bioinformatic and statistical analysis**

284

285 Initially the forward and reverse reads were taken and merged together using the PEAR
286 Illumina paired-end read merger (Zhang et al., 2014). Reads were then filtered for quality by
287 trimming them once average quality dropped below 25 and prefix dereplication was
288 performed using the USEARCH algorithm (Edgar, 2010). Sequences below 100bp were not
289 written to the output file and no minimum cluster size restriction was applied. Clustering was
290 performed at a 4% divergence using the USEARCH clustering algorithm (Edgar, 2010).
291 Clusters containing less than 2 members were removed. OTU selection was performed using
292 the UPARSE OTU selection algorithm (Edgar, 2013). Chimeras were then checked for and
293 removed from the selected OTUs using the UCHIME chimera detection software executed in
294 *de novo* mode (Edgar et al., 2011). Reads were then mapped to their corresponding
295 nonchimeric cluster using the USEARCH global alignment algorithm (Edgar, 2010). The
296 denoised sequences were demultiplexed and the primer sequences removed. These sequences
297 were then clustered into OTUs using the UPARSE algorithm (Edgar, 2013) which assigns
298 each of the original reads back to their OTUs and writes the mapping data to an OTU table
299 file. The centroid sequence from each OTU cluster was then run against the USEARCH
300 global alignment algorithm and the taxonomic identification was done using a NCBI database
301 as described in Bokulich, et al. (2015). Finally, the OTU table output from sequence
302 clustering was collated with the output generated during taxonomic identification and a new
303 OTU table with the taxonomic information tied to each cluster was created (Bokulich et al.,
304 2015).

305

306 **2.7. Protein identification and quantification**

307

308 All MS and MS/MS raw spectra were processed using Data Analysis 4.1 software (Bruker,
309 Germany) and the spectra from each Bruker analysis file were output as a mascot generic file
310 (MGF) for subsequent database searches using Mascot Daemon (version 2.5.1, Matrix
311 Science, USA). The peptide spectra were searched against a eukaryotic and a prokaryotic
312 database created by collating all Uniprot entries (retrieved on 24 February 2015) from
313 organisms with an abundance of > 1% in the 16 and 18S rDNA survey of our inoculum
314 (Table 1, full list in Supp. Mat. Table 2 and 3). This search was undertaken utilizing the two-
315 step approach described in Jagtap et al., 2013. Briefly, the initial database search was done
316 without any false discovery rate (FDR) limitation and then was followed by a second search
317 with a 1% FDR threshold against a refined database created by extracting the protein
318 identifications derived from the first search. FDRs for assigning a peptide match were
319 determined from the ratio of the number of peptides that matched to the reversed sequence
320 eukaryotic and prokaryotic databases to the number of peptides matched to the same
321 databases in the forward sequence direction. The following search parameters were applied to
322 both searches: up to one missed cleavage with trypsin, fixed modification of cysteine residues
323 by carbamidomethylation, variable modification of methionine by oxidation, instrument
324 specification ESI Q-ToF, peptide charge: 2+, 3+ and 4+, precursor mass tolerance of ± 0.2 Da
325 and fragment-ion mass tolerance of ± 0.02 Da. For the second search only matches above a
326 95% confidence homology threshold, with significant scores defined by Mascot probability
327 analysis, and a 1% FDR cut-off were considered confidently matched peptides. 'Show sub-
328 sets' and 'require bold red' were applied on initial Mascot results to eliminate redundancy.
329 The highest score for a given peptide mass (best match to that predicted in the database) was
330 used to identify proteins, which in turn were assigned a most probable host. Furthermore,
331 only when two or more unique peptides, per protein, were matched did we consider a protein
332 identified. Protein abundance was relatively estimated through the exponentially modified
333 protein abundance index (emPAI) (Ishihama et al., 2005). emPAI is an approximate, label-
334 free, relative quantitation of the proteins. This method is based on the protein abundance

335 index (PAI) that calculates the number of different observed peptides divided by the number
336 of observable peptides as a measure of abundance. This PAI value is then exponentially
337 modified to derive the emPAI score. A protein abundance is then finally calculated after
338 normalizing the emPAI score for a protein by dividing it by the sum of the emPAI scores for
339 all identified proteins (Ishihama et al., 2005).

340

341 **2.8. Functional classification of proteins**

342

343 Proteins were semi-automatically attributed a functional classification. Briefly, a list of
344 UniProt accession numbers was collated from each sample and queried utilizing the UniProt
345 Retrieve/ID mapping tool (<http://www.uniprot.org/uploadlists/>). Column options 'Keywords'
346 and 'Gene ontology (biological process)' were selected. Incomplete or ambiguous
347 annotations were then manually completed by searching for the individual UniProt accession
348 numbers on Pfam (<http://pfam.xfam.org/>) and EggNOG (<http://eggnogdb.embl.de/>).

349

350 **3. Results and discussion**

351

352 **3.1. Biological and physicochemical measurements**

353

354 The time points chosen for metaproteomic analysis of our samples were based on biological
355 and physicochemical variables measured in our microcosms. Algal and cyanobacterial
356 abundance peaked at day three, and was maintained until nitrate and phosphate
357 concentrations were no longer in detectable range, but declined after their depletion between
358 days six and eight (Fig. 1). The decline in abundance of algae and cyanobacteria was
359 followed by a peak of bacterial abundance at day 12 (Fig. 1). Heterotrophic bacterial growth
360 is known to be stimulated by an accumulation of dissolved organic matter (DOM) derived
361 from senescent algae and cyanobacteria. Hence, in a given body of water the peak of
362 heterotrophic bacterial activity tends to follow the peak of primary production.

363

364 Based on these patterns the samples selected for metaproteomic analyses were harvested at
365 day three, the peak of algal and cyanobacterial concentrations, (early oligo- and eutrophic)
366 and day 12, the peak of bacterial concentrations, (late oligo- and eutrophic). The comparative
367 analysis of these biologically distinct time points can provide information regarding the
368 activity of the microbial community during algal/cyanobacterial dominance and bacterial
369 dominance under low and high nutrient conditions.

370

371 Similar patterns were observed in DO, pH and temperature measurements in both nutrient
372 treatments (Supp. Mat. Fig. 1) and together with the low level of variation observed in
373 biological measurements (Fig.1), provided additional confidence in the sample pooling
374 approach for metaproteomics analyses.

375

376 **3.2. Metaproteomic database creation and search results**

377

378 The 18S rDNA sequencing of the microcosm inoculum indicated that, at day 0, the
379 eukaryotic community was predominantly composed of Chlorophyceae (e.g. Chloromonas)
380 and Bacillariophyceae (e.g. Stephanodiscus) and Chrysophyceae (e.g. Chromulinaceae).
381 These are typical unicellular freshwater microalgal species that are normally found in
382 freshwater oligotrophic environments (Bailey-Watts, 1992).

383

384 The 16S rDNA sequencing of the microcosm inoculum showed that, at day 0, the prokaryotic
385 community was predominantly composed of Alpha-proteobacteria (e.g. *Brevundimonas*),
386 Beta-proteobacteria (e.g. *Rhodospirillum rubrum*), Flavobacteria (e.g. *Flavobacterium*) and
387 Cyanophyceae (e.g. *Anabaena*). Proteobacteria and Flavobacteria are ubiquitous in
388 freshwater environments with the latter being known to dominate eutrophic environments
389 where phytoplankton population numbers are high (Eiler and Bertilsson, 2007; Newton et al.,
390 2011). *Anabaena* is a well-researched freshwater cyanobacterium that is known to
391 occasionally be responsible for harmful algal blooms (Elser et al., 2007).

392

393 This list of organisms was utilized to create a eukaryotic and a prokaryotic protein database
394 by collating all Uniprot entries from organisms with an abundance of > 1% in the 16 and 18S
395 rDNA survey of the inoculum (Table 1; full list in Supp. Mat. Table 2 and 3). This approach
396 was applied to limit the size of the resulting protein databases, which can lead to high false
397 positive rates, and also in accordance with the nature of mass spectrometry based proteomics,
398 where only the most abundant proteins are identified. As a result the eukaryotic and
399 prokaryotic databases contained 86336 and 350356 sequence entries, respectively. These
400 databases were utilized to identify proteins from peptide fragments in a two-step approach
401 (Jagtap et al., 2013). This approach is valuable when dealing with large metaproteomic
402 database searches where the target and decoy identifications may overlap significantly and
403 valuable identifications are missed out (Muth et al., 2015). Proteins of eight samples,
404 representing the two time points selected under different nutrient concentrations (early and
405 late oligo- and eutrophic) and two size separated fractions, (free-living bacteria (<3 µm in
406 size) and algae/particle-associated bacteria (> 3 µm in size)) were identified and an average
407 of 131 ± 28 proteins, above a 95% confidence homology threshold, a 1% FDR cut-off and
408 with two unique peptides, were identified per sample. Values were pooled by broad protein
409 annotation and taxonomic categories to evaluate differences between early and late
410 oligotrophic and eutrophic conditions. The average coefficient of variation (CV) of emPAI
411 across three biological replicates in non-fractionated protein samples, was 0.15. The average
412 relative variance (RV) was also determined logarithmically and was 0.82 indicating a 18%
413 discrepancy for relative quantitation. This provided us with confidence of a 1.5 fold cut off to
414 minimize the identification of false positive differentially regulated proteins.

415

416

417 **3.3. Phylogenetic diversity according to the metaproteomic spectra**

418

419 Identifying discrepancies between the phylogenetic classification of the identified proteins
420 and the 16 and 18S rDNA sequencing used to create the metaproteomic database can indicate
421 if any specific phylogenetic group is inadequately represented. rDNA sequencing was
422 performed on the inoculum (i.e. at day 0 of the experiment) and therefore a direct comparison
423 with the metaproteomes is not possible. Nevertheless, the 16 and 18S rDNA sequencing
424 information provided a template to which the metaproteome could be compared. Of the total
425 number of identified proteins in the >3 µm fraction, across all four samples, 48-55% were
426 identified in Chlorophyta, 9-27% in Heterokontophyta and, finally, 12-33% in Cyanobacteria.

427

428 A more detailed look at the genus level of the phylogenetic distribution showed that
429 *Chlamydomonas* sp. proteins are most abundant in the early part of the time series
430 (oligotrophic (50%) and eutrophic (43%)), *Chlorella* sp. in late oligotrophic (39%) and
431 *Anabaena* sp. in late eutrophic (37%) conditions. The 18S rDNA sequencing indicated that
432 the abundance of the *Chlorella* genus was only 1.08% of the initial inoculum. However,
433 proteins belonging to the *Chlorella* genus represented up to 39% of total protein. This is most

434 likely due to an over representation of *Chlorella* sp. in the metaproteomic database due to it
435 being a model genus with a large number of sequences available in Uniprot.

436

437 The phylogenetic distribution, based on proteins identified across the samples, mostly fitted
438 with the biological measurements. Microalgae concentrations were always higher than
439 cyanobacteria concentrations over the course of the experiment (Fig. 1). Cyanobacteria had
440 the highest number of proteins identified in late eutrophic (37%) mostly due to the expression
441 of highly abundant proteins related to carbon concentration mechanisms. It has been
442 suggested that this is a mechanism of survival under adverse conditions that could, in the long
443 term, favor cyanobacterial populations (Yeates et al., 2008).

444

445 Of the total number of identified proteins in the <3 μm fraction, across all four samples, 60-
446 73% were identified in Proteobacteria (60-73%) and 27-40% in Bacteroidetes. Bacteroidetes
447 proteins were more abundant in early oligotrophic conditions whereas Proteobacteria were
448 more abundant in late oligotrophic and early eutrophic conditions. A more detailed look at
449 the class level of the phylogenetic distribution showed that Flaviobacteria proteins were more
450 abundant in the early phase (oligotrophic (29%) and eutrophic (30%)) while Alpha-
451 proteobacteria proteins were abundant in late oligotrophic (30%) and Beta-proteobacteria
452 proteins in late eutrophic (30%) conditions.

453

454 Again, the taxonomic community composition found by 16S rDNA sequencing and the
455 metaproteome were in agreement and the phylogenetic distribution across the samples
456 supports previous observations of these organisms. Flaviobacteria typically establish
457 mutualistic relationships with algae on the cell surface and are more abundant when algal
458 concentrations are high such as earlier in the time series (Fig. 1a). Alpha-proteobacteria and
459 Beta-proteobacteria, as opportunistic heterotrophs, therefore thrive in the presence of DOM
460 derived from algal and cyanobacterial decay which was abundant later in the time series (Fig.
461 1a, b) (Teeling et al., 2012).

462

463 **3.4. Functional classification of proteins**

464

465 The distribution of identified proteins by their functional classification resulted in 20 distinct
466 functional categories. The grouping of proteins identified in each fraction and nutrient
467 condition can give an overview of how the community function differed over time and
468 nutrient enrichment.

469

470 Of the total number of identified proteins, 25% were involved in photosynthesis, thus,
471 dominating the >3 μm fraction (Fig. 2). 9% of the total protein library were classified with
472 unknown function. Proteins with assigned functions in each individual samples were
473 dominated by photosynthesis (early oligotrophic, 21%; late oligotrophic, 25%; early
474 eutrophic, 26%; late eutrophic, 30%). On the individual protein level, photosystem II (PSII)
475 CP43 reaction center proteins were the most abundant in early oligotrophic (8%), histone H2
476 proteins in late oligotrophic (14%), PSII CP43 reaction center proteins and histone H4
477 proteins (8% each) in early eutrophic and microcompartment proteins (16%) in late eutrophic
478 conditions.

479

480 In agreement with our findings, Hanson et al. (2014) observed that in both freshwater and
481 marine surface samples (i.e. rich in primary production) there was widespread evidence of
482 photosynthesis (e.g. PSII) and carbon fixation (e.g. ribulose-1,5-bisphosphate carboxylase

483 oxygenase (RuBisCO) (EC 4.1.1.39). Although our samples were not rich in RuBisCO, the
484 presence of microcompartment proteins are evidence of carbon fixation.

485

486 Of the total number of identified proteins, transport (12%) and translation (12%) proteins
487 were predominant in the <3 μm fraction (Fig. 3). A more detailed view showed early
488 oligotrophic conditions dominated by transport proteins (12%), late oligotrophic by
489 translation proteins (18%), early eutrophic by transcription proteins (19%) and late eutrophic
490 by stress response proteins (16%). On the individual protein level the ATP-binding cassette
491 (ABC) transporter proteins were the most abundant in early oligotrophic (5%), elongation
492 factor proteins in late oligotrophic (16%), DNA-directed RNA polymerase subunit beta (EC
493 2.7.7.6) in early eutrophic (19%) and ABC transporter proteins (7%) in late eutrophic
494 conditions. Proteins involved in transport (e.g. ABC transporters), translation (e.g. elongation
495 factors) and transcription (DNA-directed RNA polymerase subunit beta) are amongst the
496 most commonly identified proteins in environmental samples (Ng et al., 2010; Sowell et al.,
497 2011b; Hanson et al., 2014).

498

499 **3.5. Metaproteomic analysis of microcosm microbial activity**

500

501 Having identified protein functional groups in eukaryotic and prokaryotic organisms
502 throughout our samples, we can now assess functional differences between oligotrophic and
503 eutrophic conditions, early and late in the time series. We found several patterns previously
504 documented and several unexpected differences between time points and between
505 oligotrophic and eutrophic conditions within each time point. Fig. 4 captures a summary of
506 the functional differences among the times and treatments, and we now refer to this figure,
507 and Figs. 2 and 3, to provide detail.

508

509 First, virtually all the photosynthesis and carbon fixation proteins were identified in
510 *Anabaena* sp., *Chlamydomonas* sp. and *Chlorella* sp. This is similar to previous
511 metaproteomic studies where the freshwater surface is typically rich in photosynthetic
512 organisms (Hanson et al., 2014). The most abundant of the two categories was photosynthesis
513 (emPAI = 11.89) and it represented 40% of all proteins expressed by photoautotrophic
514 organisms. The majority of the proteins were components of PSII (e.g. reaction center
515 components). This was expected because PSII proteins are 40% to 90% more abundant than
516 PSI proteins and are the most abundant membrane proteins in algae and cyanobacteria
517 (Nobel, 2005). Photosynthetic proteins were abundant in both timepoints (early, emPAI =
518 5.27 and late, emPAI = 5.61) and in both nutrient treatments (oligotrophic, emPAI = 5.31 and
519 eutrophic, emPAI = 5.57), suggesting that the phototrophs are demanding a constant energy
520 supply, even outside of the exponential growth phase.

521

522 Second, amongst the photosynthetic microbes, there is interest in identifying mechanisms that
523 could potentially favor cyanobacteria in eutrophic conditions. The increase in the number of
524 nutrient enriched water bodies has led to issues with freshwater quality and the proliferation
525 of harmful cyanobacteria (O'Neil et al., 2012). There have been numerous proteomics studies
526 of toxic bloom causing cyanobacteria that have focused on the molecular mechanisms of pure
527 cultures. For example, a study of the proteomes of six toxic and nontoxic strains of
528 *Microcystis aeruginosa* linked nitrogen regulation to toxicity (Alexova et al., 2011) and
529 another study, of *Anabaena* sp. Strain 90, linked phosphorus starvation to the down
530 regulation of the Calvin cycle and amino-acid biosynthesis (Teikari et al., 2015). Studies such
531 as these provide valuable information regarding species in isolation, however,

532 metaproteomics can go a step further and contextualize these findings within the microbial
533 community structure and dynamics.

534

535 Our microcosm data showed that pigment proteins in *Anabaena* sp. were less abundant in
536 oligotrophic than in eutrophic conditions (oligotrophic, emPAI = 0.42; eutrophic, emPAI =
537 0.96). A similar pattern was found for cyanobacterial proteins with roles in carbon fixation
538 (oligotrophic, emPAI = 0.14; eutrophic, emPAI = 2.03). Cyanobacteria have the ability to
539 adapt to different environments by adjusting their light harvesting abilities (i.e. increase in
540 pigments) and carbon fixation mechanisms. However these adaptation processes can be
541 hampered by insufficient nutrient supply (Tilzer, 1987). Grossman et al. (1993) showed that
542 during nutrient starvation, there is a rapid degradation of the phycobilisome. Phycobilisome
543 degradation can provide nutrient-starved cells with amino acids used for the synthesis of
544 proteins important for their metabolism (Grossman et al., 1993). This suggests that nutrient
545 enrichment would allow cyanobacteria to increase pigment numbers, thus increasing light
546 harvesting ability, and outcompete algal species in eutrophic conditions (Tilzer, 1987).

547

548 Regarding carbon fixation, microcompartment proteins were identified in *Anabaena* sp. and
549 were only found in in late eutrophic conditions (eutrophic, emPAI = 1.52).

550 Microcompartments sequester specific proteins in prokaryotic cells and are involved in
551 carbon concentrating mechanisms (CCMs) in low CO₂ conditions. The carboxysome, a
552 bacterial microcompartment that is found in cyanobacteria and some chemoautotrophs,
553 encapsulates RuBisCO and carbonic anhydrase (EC 4.2.1.1) The carbonic anhydrase
554 reversibly catalyzes the conversion of bicarbonate into carbon dioxide within the
555 carboxysome therefore acting both as a intracellular equilibrators and a CO₂ concentrating
556 mechanism (Yeates et al., 2008). However, no carbonic anhydrases were identified in our
557 dataset. A higher abundance of carbon fixation proteins in *Anabaena* sp., in eutrophic
558 conditions, indicates that carbon requirement was higher, likely matching higher
559 photosynthesis rates compared to the oligotrophic conditions, where low nitrogen and
560 phosphorus concentrations are likely limiting factors and therefore, not allowing the
561 population to reach a point of carbon limitation.

562

563 Finally, carbon fixation proteins in *Chlamydomonas* sp. were also more abundant in eutrophic
564 conditions (oligotrophic, emPAI = 0.17; eutrophic, emPAI = 0.40). The proteins identified
565 were mainly involved in the Calvin cycle (i.e. RuBisCO), however, unexpectedly, a low-CO₂
566 inducible protein (LCIB) was identified. The LCIB is located around the pyrenoid and traps
567 CO₂, either from escaping from the pyrenoid or entering from outside the cell, into the
568 stromal bicarbonate pool thus, functioning as a CCM (Wang and Spalding, 2014). Wang and
569 Spalding hypothesized that this system may reflect a versatile regulatory mechanism present
570 in eukaryotic algae for acclimating quickly to changes in CO₂ availability that frequently
571 occur in their natural environments. The possibility of switching between an energy-intensive
572 bicarbonate transport system (low CO₂) and diffusion based CO₂ uptake system (high CO₂)
573 that may be energetically less costly, would enable faster growth at a lower energy cost.

574

575 These observations suggest that algae and cyanobacteria both adapt to carbon limitation
576 through an increase in carbon fixation proteins and the deployment of CCMs (e.g.
577 carboxysomes). In a low-carbon lake, the microbial population may thus fix atmospheric CO₂
578 to correct the carbon deficiency and grow in proportion to existing nitrogen and phosphorus
579 levels. This maps onto the hypothesis that carbon limitation may not be adequate for algal or
580 cyanobacterial bloom mitigation (Schindler et al., 2008).

581

582 **3.5.1. Bacterial photosynthesis and carbon fixation**

583

584 Heterotrophic bacteria are known to be responsible for the bulk of sequestration and
585 remineralization of organic matter in phytoplankton associated bacterial assemblages
586 (Buchan et al., 2014). However, the role of photoheterotrophic and chemoautotrophic
587 bacteria in these assemblages, and how they vary along environmental gradients, remains
588 under-studied (Yutin et al., 2007; Ng et al., 2010). The observations to date suggest that these
589 bacteria are ubiquitous but have a preference for carbon limiting environments such as the
590 DOM poor conditions found early in the time series, during algal and cyanobacterial
591 dominance, in this study (Fig. 4).

592

593 In support of this hypothesis, bacterial photosynthesis (i.e. magnesium chelatase (EC
594 6.6.1.1)) and carbon fixation proteins (i.e., RuBisCO, carbonic anhydrase) were identified in
595 in both treatments (Fig. 4) with predominance early in the time series (early, emPAI = 1.28;
596 late, emPAI = 0.11) and eutrophic conditions (oligotrophic, emPAI = 0.57; eutrophic, emPAI =
597 = 0.82). Specifically, in Alpha- and Beta-proteobacteria, magnesium chelatase (emPAI =
598 0.03), which is involved in bacteriochlorophyll biosynthesis, was identified in early
599 oligotrophic (emPAI = 0.03) and RuBisCO was present in both nutrient treatments. Alpha-
600 and Beta-proteobacteria include several mixotrophic species that are known to perform
601 aerobic and anaerobic respiration and use combinations of photo-, chemo-, auto- and
602 heterotrophic metabolism to adapt to different environmental conditions. Some of these
603 bacterial species perform anoxygenic photosynthesis, where light energy is captured and
604 converted to ATP without the production of oxygen, and are described as
605 photo(chemo)heterotrophs due to their requirement of organic carbon. It has been suggested
606 that these bacteria grow chemoheterotrophically but utilize light as an additional energy
607 source (Eiler, 2006).

608

609 The low levels of DOM in early oligotrophic conditions (i.e. algal and cyanobacterial
610 dominance) provided a niche for phototrophy and autotrophy. Later, in the presence of DOM
611 derived from algal and cyanobacterial cell lysis, the bacterial groups changed to a
612 heterotrophic metabolism. This suggests that an increase in Proteobacterial metabolism
613 depends more on the concentrations of organic matter than on nitrogen and phosphorus, and
614 that bacterial mixotrophy is ubiquitous in low DOM freshwater environments. This has
615 consequences for biogeochemical models such as the microbial loop. The classic separation
616 of primary and secondary producers into photoautotrophs and organoheterotrophs,
617 respectively, is no longer valid and may lead to the underestimation of bacterial biomass
618 production and their importance to higher trophic levels (Eiler, 2006).

619

620 Finally, other bacterial groups found in our study, such as the Bacteroidetes, can also use
621 non-photosynthetic routes of light-dependent energy generation. Previous metaproteomic
622 studies have shown that proteorhodopsin, a light driven proton pump, is ubiquitous in marine
623 and freshwater environments (Atamna-Ismael et al., 2008; Williams et al., 2013). Its
624 expression has been linked to survival in situations where sources of energy are limiting and
625 cells have to resort to alternative means of generating energy (González et al., 2008).
626 However, proteorhodopsin was not detected either because of non-expression in the
627 conditions tested, low abundance or low solubility of the protein; proteorhodopsin contains
628 seven transmembrane helices and is imbedded in the plasma membrane thus making it
629 difficult to solubilize and detect (Sowell et al., 2009).

630

631 **3.5.2. Bacteroidetes: an algal associated bacterial group**

632
633 The Bacteroidetes phylum has been hypothesised to specialise in degrading high molecular
634 weight (HMW) compounds and growing whilst attached to particles, surfaces and algal cells
635 (Teeling et al., 2012; Fernandez-Gomez et al., 2013; Williams et al., 2013). Teeling et al.
636 (2012) also observed that the bacterial response to a coastal algal bloom was characterized by
637 an initial surge in Bacteroidetes abundance. Thus, it was hypothesized that this group
638 colonizes the phytoplankton surface and acts as “first responders” to algal blooms (Williams
639 et al., 2013). Therefore, the identification of proteins that suggest a tight algae – bacteria
640 relationship were expected to be found early in the time series. Also, the higher algal
641 concentrations in eutrophic conditions (Fig. 1) would presumably provide a richer
642 environment for the Bacteroidetes population.

643
644 As predicted, in both oligotrophic and eutrophic treatments, Bacteroidetes proteins were
645 considerably more abundant in the early phase of the experiment (early, emPAI = 14.84, late,
646 emPAI = 5.85) with several of the identified proteins suggesting a close association with
647 algae (Fig. 4). First, several proteins attributed to the TonB-dependent transporter (TBDT)
648 system were identified. TBDTs are involved in proton motive force-dependent outer
649 membrane transport and once thought to be restricted to iron-chelating compounds (i.e.
650 siderophores) and vitamin B12 uptake. Recently TBDTs have been found to specialize in the
651 uptake of HMW compounds that are too large to diffuse via porins (e.g. polysaccharides,
652 proteins) (Blanvillain et al., 2007). In Bacteroidetes, the genes for the TBDT system are
653 located in the same gene cluster as several of the polymer capture (e.g. starch utilization
654 system) and degradation genes (e.g. glycoside hydrolases (GHs), peptidases) suggesting an
655 integrated regulation of capture, degradation and transport of complex substrates (Fernandez-
656 Gomez et al., 2013). The proteins identified in our Bacteroidetes dataset support this
657 suggestion.

658
659 Second, three starch utilization system proteins (SusD/RagB) in Bacteroidetes were identified
660 early in the time series (Fig. 4). SusD proteins are present at the surface of the cell and they
661 mediate starch-binding before transport into the periplasm for degradation. RagAB is
662 involved in binding exogenous proteins (Gilbert, 2008; Dong et al., 2014). GHs from several
663 families (GH3, GH29, GH30 and GH92), together with three peptidases (methionine
664 aminopeptidase (EC 3.4.11.18), peptidase M16, peptidyl-dipeptidase (EC 3.4.15.1)) were
665 also identified. As mentioned previously GHs are carbohydrate-active enzymes (CAZymes)
666 specialized in the uptake and breakdown of complex carbohydrates, especially algal
667 polysaccharides (Teeling et al., 2012; Mann et al., 2013). Together with peptidases these
668 enzymes are responsible for extracellular breakdown of organic matter in order to be
669 transported into the cytoplasm by the TBDT system.

670
671 Finally, the identification of proteins with cell adhesion functions (intimin, thrombospondin
672 1, gliding motility protein and YD repeat) provides further evidence that this bacterial
673 phylum specializes in surface attachment. Intimin, thrombospondin and YD repeat protein are
674 adhesive proteins that mediate cell-to-cell interactions and gliding mobility proteins allow
675 exploration of solid surfaces (McBride, 2001). Other bacterial species utilize gliding motility
676 for essential life cycle processes (e.g. swarming, predation) usually in coordinated groups but
677 also as isolated adventurous individuals (Nan and Zusman, 2011). In a similar way
678 Bacteroidetes species may use gliding motility to follow algal exudate trails and to move to
679 advantageous positions within the phycosphere, the microscale mucus region rich in organic
680 matter that surrounds algal and cyanobacterial cells. This could confer a competitive
681 advantage over free-floating bacterial species.

682
683 When contrasting oligo- and eutrophic treatments, Bacteroidetes associated proteins were,
684 unexpectedly, more abundant in oligotrophic rather than eutrophic conditions (oligotrophic,
685 emPAI = 14.02; eutrophic, emPAI = 6.67). In eutrophic conditions proteins attributed to
686 transport, macromolecule degradation, outer membrane capture and chemotaxis were
687 virtually non-existent (Fig. 4). The fact that very little capture and degradation was occurring
688 in eutrophic conditions suggests algal exudation was substantially lower. In the past, it has
689 been hypothesized that nutrient limitation is a requirement for algal and cyanobacterial
690 exudation (Wood and Van Valen, 1990; Guenet et al., 2010). Van den Meersche et al. (2004)
691 determined that contribution of algal derived DOM to the experimental ecosystem carbon
692 pool varied from ~2% (nutrient-replete early bloom) to 65% (nutrient-deplete mid-late
693 bloom). Thus, the stimulation of DOM release, by nutrient limiting conditions, paradoxically
694 provides carbon substrates for bacterial growth which then compete with the algae for
695 nutrients (Van den Meersche et al., 2004). Therefore, the survival of Bacteroidetes
696 populations seems to be linked to environmental conditions and the physiological state of
697 neighboring algae.

698 699 **3.5.3. ABC transporters reveal ecological niches**

700
701 In Alpha- and Beta-proteobacteria ATP-binding cassette (ABC) transporters were the most
702 prevalent transport proteins identified (Fig. 4). This is in agreement with previous freshwater
703 and marine metaproteomic studies (Ng et al., 2010; Teeling et al., 2012; Georges et al.,
704 2014). The majority of the ABC transporters were periplasmic-binding proteins (PBPs). The
705 high representations of PBPs is commonly observed in aquatic metaproteomic studies. These
706 subunits are far more abundant than the ATPase or permease components of ABC
707 transporters in order to increase the frequency of substrate capture. Membrane proteins (e.g.
708 permeases) are also inherently difficult to extract and solubilize therefore reducing the
709 frequency of their detection (Williams and Cavicchioli, 2014).

710
711 In a metaproteomic comparison of Atlantic Ocean winter and spring microbial plankton,
712 Georges et al. (2014) found ABC transporters were more abundant in low nutrient surface
713 waters in mid-bloom and were mostly specific for organic substrates. Therefore, these type of
714 transporters may be expected to more prevalent in the early oligotrophic conditions of our
715 study where bacterial levels were higher (Fig. 1B) and the environment was rich in algal and
716 cyanobacterial exudate (discussed in previous section). As expected, transporter proteins in
717 Alpha- and Beta-proteobacteria were more abundant in oligotrophic than eutrophic conditions
718 (emPAI = 3.32 and emPAI = 1.73, respectively). They were predominant in early phase in
719 oligotrophic (early, emPAI = 1.42 and late, emPAI = 0.9) and late phase in eutrophic
720 conditions (early, emPAI = 0.42 and late, emPAI = 0.88). Furthermore, in both treatments
721 and timepoints the majority of ABC transporters were specific for organic substances (i.e.
722 carbohydrates and amino acids). This suggests that both proteobacterial phyla are specialized
723 in obtaining nutrients from DOM therefore investing more resources in the acquisition of
724 organic rather than inorganic substrates and were favored in early oligotrophic when the rate
725 of algal exudation was potentially higher (Teeling et al., 2012).

726
727 Finally, another particularity of ABC transporters is that the expression of these transporters
728 comes at an additional metabolic cost and therefore they are mainly synthesized to target
729 substrates that are limiting in the environment. Thus, determining which transporters are
730 being expressed can provide clues to which substrate is limiting. There was a clear difference
731 in substrate preference between the two (Fig. 4); *Rhodobacter* sp. (Alpha-proteobacteria)

732 carbohydrate transporter expression was more than two-fold higher than amino acid
733 transporter expression (carbohydrate, emPAI = 0.57; amino acid, emPAI = 0.21) whereas in
734 the bacterial group *Hydrogenophaga* sp. (Beta-proteobacteria) only amino acid transporter
735 expression was observed (carbohydrate, emPAI = 0.00; amino acid, emPAI = 0.81). This has
736 been previously observed (Schweitzer et al., 2001; Pérez et al., 2015) and is a case of
737 resource partitioning, a mechanism through which two phylogenetic groups can co-exist in
738 the same environment without leading to competitive exclusion (Morin, 2011).

739

740 **4. Conclusions**

741

742 A label-free comparative metaproteomics approach was applied on an experimental
743 microcosm community under differing trophic states. The identification of proteins in early
744 and late oligo- and eutrophic conditions allowed us to link function to phylogenetic diversity
745 and reveal individual transitional niches. The results from this study also compared favorably
746 with many *in situ* aquatic metaproteomic studies.

747

748 Algae and cyanobacteria predominantly expressed, as would be expected, proteins related to
749 photosynthesis and carbon fixation. Interestingly, proteins involved in mechanisms of carbon
750 concentration were abundant in virtually all samples, which indicated that carbon could be a
751 limiting factor throughout the experiment. The fact that cyanobacteria, in eutrophic
752 conditions, expressed several proteins related to environmental adaptation (e.g.
753 microcompartment proteins) suggests that they may be better equipped than algal species to
754 dominate nutrient enriched environments.

755

756 Proteins identified in all bacterial species suggested an alignment with oligotrophic
757 environments. In early oligotrophic, Bacteroidetes showed characteristics that suggest a role
758 as a fast-growing population that is specialized in cell and particle attachment and are the first
759 to respond to algal growth. This ecosystem role can coexist with bacterial heterotrophs that
760 live suspended in the water column and depend on algal exudate and decaying organic
761 matter. ABC transporters were amongst the most abundant proteins identified. In a case of
762 resource partitioning it was found that Alpha- and Beta-proteobacteria co-exist and
763 metabolize algal/cyanobacterial exudate, but the former will preferentially uptake
764 carbohydrates whereas the latter will prefer amino acid uptake thus avoiding direct
765 competition. There is the evidence that bacterial metabolism controls primary production
766 through the remineralization of nutrients, however, here it is shown that primary producers
767 can also be a driver of bacterial community composition and function.

768

769 This study successfully showed that microcosms can be used to observe microbial
770 mechanisms that are typical of the natural environment. While these microcosm systems are
771 simplified, and may not completely represent global biogeochemical cycles, they can
772 accurately provide a snapshot of a microbial community in controlled conditions, and offer
773 the potential to employ more manipulative experimentation to uncover functions and
774 processes in oligo- and eutrophic conditions. The study also demonstrated that a community
775 metagenetic analysis can provide a usable database for high mass accuracy metaproteomics
776 studies. Ultimately, these data suggest that nutrient enrichment affected the dynamics of
777 individual microbes and how they interact with others in their vicinity. Further manipulative
778 experiments and associated 'omics methodology will significantly contribute to our
779 understanding of how microbial communities adapt to local environmental conditions.

780

781 **Funding**

782
783 Natural Environment Research Council and Technology Strategy Board [NE/J024767/1].
784

785 **Acknowledgements**

786
787 DR thanks Benjamin Strutton, Thomas Minshull, Mark Jones and the Groundwater
788 Protection and Restoration group who assisted with sample collection and analyses, Joseph
789 Longworth for assistance with database creation and search, Julie Zedler for valuable
790 comments to the manuscript and Phillip Warren for constructive discussions on microcosm
791 design.

792 **Conflict of interest**

793
794
795 The authors declare that the research was conducted in the absence of any commercial or
796 financial relationships that could be construed as a potential conflict of interest.

797 **Author contribution statement**

798
799
800 This study was designed and coordinated by DR, AB and JP. JP, as principal investigator,
801 and AB provided technical and conceptual guidance for all aspects of the project. DR planned
802 and undertook all the practical aspects of the manuscript. NC contributed to performing and
803 analyzing all aspects of protein extraction and analysis. The manuscript was written by DR
804 and commented on by all authors.

805 **References**

806
807
808 Table 1. List of the eukaryotic and prokaryotic organisms in the experimental freshwater
809 microbial community inoculum, with an abundance higher than 1%, as determined by 16 and
810 18S rDNA sequencing. These organisms were used to guide creation of a protein database.
811

Eukaryotic organisms	%	Prokaryotic organisms	%
<i>Chloromonas pseudoplatyrhyncha</i>	26.93	<i>Rhodofera</i> sp	21.94
<i>Stephanodiscus</i> sp	18.17	Unsequenced organisms	17.84
Unsequenced organisms	17.87	<i>Flavobacterium</i> sp	9.43
<i>Chromulinaceae</i> sp	8.48	<i>Anabaena</i> sp	8.85
<i>Synedra angustissima</i>	4.99	<i>Brevundimonas diminuta</i>	4.20
<i>Ochromonadales</i> sp	3.01	<i>Hydrogenophaga</i> sp	3.41
<i>Chlamydomonas</i> sp	2.98	<i>Runella limosa</i>	2.47
<i>Micractinium pusillum</i>	1.62	<i>Haliscomenobacter</i> sp	2.43
<i>Chlorella</i> sp	1.08	<i>Rhodobacter</i> sp	2.34
<i>Pythiaceae</i> sp.	1.07	<i>Planktophila limnetica</i>	2.13
		<i>Agrobacterium tumefaciens</i>	2.11
		<i>Sphingobacterium</i> sp	2.03
		<i>Ochrobactrum tritici</i>	1.98
		<i>Brevundimonas variabilis</i>	1.83
		<i>Sphingomonas</i> sp	1.73
		<i>Curvibacter</i> sp	1.48
		<i>Phenylobacterium falsum</i>	1.42

Roseomonas stagni 1.24
Oceanicaulis sp 1.03

812

813

Provisional

814 **Figure legends**

815

816 Figure 1. Time series of the measured variables in the oligotrophic and eutrophic treatments.
817 Top: Chlorophyll *a* and cyanobacterial fluorescence. Middle: culturable heterotrophic
818 bacteria. Bottom: NO₃⁻ and PO₄³⁻. Error bars show standard errors (n = 3).

819

820 Figure 2. Comparison across samples of the distribution of identified proteins by their
821 functional classification in the >3 μm fraction.

822

823 Figure 3. Comparison across samples of the distribution of identified proteins by their
824 functional classification in the <3 μm fraction.

825

826 Figure 4. Depiction of the metabolic characteristics of oligotrophic and eutrophic
827 communities inferred from the metaproteome. Red and blue squares depict algal and
828 cyanobacterial exudate (red, sugars; blue, amino acids). Grey algae and cyanobacteria depict
829 senescent cells. Structures and processes that are hypothesised to be present, albeit with no
830 direct evidence from our dataset, are depicted with a dashed line. ABC, ATP-binding cassette
831 transporter; GHs, glycoside hydrolases; GM, gliding motility; HMW, high molecular weight
832 compounds; N₂ fix, nitrogen fixation; TBDT, Ton-B-dependent transporter.

833

834

835

836 Aebersold, R., Hood, L.E., and Watts, J.D. (2000). Equipping scientists for the new biology.
837 *Nat Biotechnol* 18, 359. doi: 10.1038/74325.

838 Alexova, R., Haynes, P.A., Ferrari, B.C., and Neilan, B.A. (2011). Comparative protein
839 expression in different strains of the bloom-forming cyanobacterium *Microcystis*
840 *aeruginosa*. *Mol Cell Proteomics* 10, M110 003749. doi: 10.1074/mcp.M110.003749.

841 Atamna-Ismaeel, N., Sabehi, G., Sharon, I., Witzel, K.-P., Labrenz, M., Jurgens, K., Barkay,
842 T., Stomp, M., Huisman, J., and Beja, O. (2008). Widespread distribution of
843 proteorhodopsins in freshwater and brackish ecosystems. *ISME J* 2, 656-662.

844 Azam, F., Fenchel, T., Field, J.G., Gray, J.S., Meyer-Reil, L.A., and Thingstad, F. (1983).

845 The ecological role of water-column microbes in the sea. *Marine Ecology - Progress*
846 *Series* 10, 257 - 263.

847 Azam, F., and Malfatti, F. (2007). Microbial structuring of marine ecosystems. *Nat Rev*
848 *Microbiol* 5, 782-791. doi: 10.1038/nrmicro1747.

849 Bailey-Watts, A.E. (1992). Growth and reproductive strategies of freshwater phytoplankton.
850 *Trends in Ecology & Evolution* 4, 359. doi: 10.1016/0169-5347(89)90095-5.

851 Beutler, M., Wiltshire, K.H., Meyer, B., Moldaenke, C., Luring, C., Meyerhofer, M., Hansen,
852 U.-P., and Dau, H. (2002). A fluorometric method for the differentiation of algal
853 populations *in vivo* and *in situ*. *Photosynthesis Research* 72, 39-53.

854 Blanvillain, S., Meyer, D., Boulanger, A., Lautier, M., Guynet, C., Denance, N., Vasse, J.,
855 Lauber, E., and Arlat, M. (2007). Plant carbohydrate scavenging through tonB-

856 dependent receptors: a feature shared by phytopathogenic and aquatic bacteria. *PLoS*
857 *One* 2, e224. doi: 10.1371/journal.pone.0000224.

858 Bokulich, N., Rideout, J., Kopylova, E., Bolyen, E., Patnode, J., Ellett, Z., McDonald, D.,
859 Wolfe, B., Maurice, C., Dutton, R., Turnbaugh, P., Knight, R., and Caporaso, J.

860 (2015). A standardized, extensible framework for optimizing classification improves
861 marker-gene taxonomic assignments. *PeerJ PrePrints* 3. doi:

862 <https://doi.org/10.7287/peerj.preprints.934v2>.

863 BSI (2004). "BS EN ISO 6878:2004: Water quality. Determination of phosphorus.
864 Ammonium molybdate spectrometric method". (London: British Standards
865 Institution).

866 Buchan, A., LeClerc, G.R., Gulvik, C.A., and Gonzalez, J.M. (2014). Master recyclers:
867 features and functions of bacteria associated with phytoplankton blooms. *Nat Rev*
868 *Micro* 12, 686-698. doi: 10.1038/nrmicro3326.

869 CSLC (2009). "Assessment of the efficacy, availability and environmental impacts of ballast
870 water treatment systems for use in California waters". (California: California State
871 Lands Commission).

872 Dong, H.-P., Hong, Y.-G., Lu, S., and Xie, L.-Y. (2014). Metaproteomics reveals the major
873 microbial players and their biogeochemical functions in a productive coastal system
874 in the northern South China Sea. *Environmental Microbiology Reports* 6, 683-695.
875 doi: 10.1111/1758-2229.12188.

876 Drake, J.M., and Kramer, A.M. (2011). Mechanistic analogy: how microcosms explain
877 nature. *Theoretical Ecology* 5, 433-444. doi: 10.1007/s12080-011-0134-0.

878 Eaton, A.D., and Franson, M.A.H. (2005). *Standard Methods for the Examination of Water &*
879 *Wastewater*. American Public Health Association.

880 Edgar, R.C. (2010). Search and clustering orders of magnitude faster than BLAST.
881 *Bioinformatics* 26, 2460-2461. doi: 10.1093/bioinformatics/btq461.

882 Edgar, R.C. (2013). UPARSE: highly accurate OTU sequences from microbial amplicon
883 reads. *Nat Meth* 10, 996-998. doi: 10.1038/nmeth.2604
884 [http://www.nature.com/nmeth/journal/v10/n10/abs/nmeth.2604.html#supplementary-](http://www.nature.com/nmeth/journal/v10/n10/abs/nmeth.2604.html#supplementary-information)
885 [information](http://www.nature.com/nmeth/journal/v10/n10/abs/nmeth.2604.html#supplementary-information).

886 Edgar, R.C., Haas, B.J., Clemente, J.C., Quince, C., and Knight, R. (2011). UCHIME
887 improves sensitivity and speed of chimera detection. *Bioinformatics* 27, 2194-2200.
888 doi: 10.1093/bioinformatics/btr381.

889 Eiler, A. (2006). Evidence for the ubiquity of mixotrophic bacteria in the upper ocean:
890 Implications and consequences. *Applied and Environmental Microbiology* 72, 7431-
891 7437.

892 Eiler, A., and Bertilsson, S. (2007). Flavobacteria blooms in four eutrophic lakes: Linking
893 population dynamics of freshwater bacterioplankton to resource availability. *Applied*
894 *and Environmental Microbiology* 73, 3511-3518.

895 Elser, J.J., Bracken, M.E., Cleland, E.E., Gruner, D.S., Harpole, W.S., Hillebrand, H., Ngai,
896 J.T., Seabloom, E.W., Shurin, J.B., and Smith, J.E. (2007). Global analysis of
897 nitrogen and phosphorus limitation of primary producers in freshwater, marine and
898 terrestrial ecosystems. *Ecol Lett* 10, 1135-1142. doi: 10.1111/j.1461-
899 0248.2007.01113.x.

900 Falkowski, P., Scholes, R.J., Boyle, E., Canadell, J., Canfield, D., Elser, J., Gruber, N.,
901 Hibbard, K., Höglberg, P., Linder, S., Mackenzie, F.T., Moore III, B., Pedersen, T.,
902 Rosenthal, Y., Seitzinger, S., Smetacek, V., and Steffen, W. (2000). The global
903 carbon cycle: A test of our knowledge of earth as a system. *Science* 290, 291-296. doi:
904 10.1126/science.290.5490.291.

905 Fernandez-Gomez, B., Richter, M., Schuler, M., Pinhassi, J., Acinas, S.G., Gonzalez, J.M.,
906 and Pedros-Alio, C. (2013). Ecology of marine Bacteroidetes: a comparative
907 genomics approach. *ISME J* 7, 1026-1037. doi: 10.1038/ismej.2012.169.

908 Geissmann, Q. (2013). OpenCFU, a new free and open-source software to count cell colonies
909 and other circular objects. *PLoS One* 8, e54072. doi: 10.1371/journal.pone.0054072.

910 Georges, A.A., El-Swaiss, H., Craig, S.E., Li, W.K., and Walsh, D.A. (2014). Metaproteomic
911 analysis of a winter to spring succession in coastal northwest Atlantic Ocean
912 microbial plankton. *ISME J* 8, 1301-1313. doi: 10.1038/ismej.2013.234.

- 913 Gilbert, H.J. (2008). Sus out sugars in. *Structure* 16, 987-989. doi: 10.1016/j.str.2008.06.002.
- 914 Giovannoni, S.J., Bibbs, L., Cho, J.-C., Stapels, M.D., Desiderio, R., Vergin, K.L., Rappe,
915 M.S., Laney, S., Wilhelm, L.J., Tripp, H.J., Mathur, E.J., and Barofsky, D.F. (2005).
916 Proteorhodopsin in the ubiquitous marine bacterium SAR11. *Nature* 438, 82-85. doi:
917 http://www.nature.com/nature/journal/v438/n7064/suppinfo/nature04032_S1.html.
- 918 González, J.M., Fernández-Gómez, B., Fernández-Guerra, A., Gómez-Consarnau, L.,
919 Sánchez, O., Coll-Lladó, M., del Campo, J., Escudero, L., Rodríguez-Martínez, R.,
920 Alonso-Sáez, L., Latasa, M., Paulsen, I., Nedashkovskaya, O., Lekunberri, I.,
921 Pinhassi, J., and Pedrós-Alió, C. (2008). Genome analysis of the proteorhodopsin-
922 containing marine bacterium *Polaribacter* sp. MED152 (Flavobacteria). *Proceedings*
923 *of the National Academy of Sciences* 105, 8724-8729.
- 924 Grossman, A.R., Schaefer, M.R., Chiang, G.G., and Collier, J.L. (1993). Environmental
925 effects on the light-harvesting complex of cyanobacteria. *Journal of Bacteriology* 175,
926 575-582.
- 927 Guenet, B., Danger, M., Abbadie, L., and Lacroix, G. (2010). Priming effect: bridging the
928 gap between terrestrial and aquatic ecology. *Ecology* 91, 2850-2861. doi: 10.1890/09-
929 1968.1.
- 930 Hanson, B.T., Hewson, I., and Madsen, E.L. (2014). Metaproteomic survey of six aquatic
931 habitats: discovering the identities of microbial populations active in biogeochemical
932 cycling. *Microb Ecol* 67, 520-539. doi: 10.1007/s00248-013-0346-5.
- 933 Hettich, R.L., Pan, C., Chourey, K., and Giannone, R.J. (2013). Metaproteomics: Harnessing
934 the power of high performance mass spectrometry to identify the suite of proteins that
935 control metabolic activities in microbial communities. *Analytical chemistry* 85, 4203-
936 4214. doi: 10.1021/ac303053e.
- 937 Ishihama, Y., Oda, Y., Tabata, T., Sato, T., Nagasu, T., Rappsilber, J., and Mann, M. (2005).
938 Exponentially modified protein abundance index (emPAI) for estimation of absolute
939 protein amount in proteomics by the number of sequenced peptides per protein. *Mol*
940 *Cell Proteomics* 4, 1265-1272. doi: 10.1074/mcp.M500061-MCP200.
- 941 Jagtap, P., Goslinga, J., Kooren, J.A., McGowan, T., Wroblewski, M.S., Seymour, S.L., and
942 Griffin, T.J. (2013). A two-step database search method improves sensitivity in
943 peptide sequence matches for metaproteomics and proteogenomics studies.
944 *Proteomics* 13, 1352-1357. doi: 10.1002/pmic.201200352.
- 945 Kalb, J., V. F., and Bernlohr, R.W. (1977). A new spectrophotometric assay for protein in
946 cell extracts. *Analytical Biochemistry* 82, 362-371.
- 947 Lauro, F.M., DeMaere, M.Z., Yau, S., Brown, M.V., Ng, C., Wilkins, D., Raftery, M.J.,
948 Gibson, J.A., Andrews-Pfannkoch, C., Lewis, M., Hoffman, J.M., Thomas, T., and
949 Cavicchioli, R. (2011). An integrative study of a meromictic lake ecosystem in
950 Antarctica. *ISME J* 5, 879-895. doi: 10.1038/ismej.2010.185.
- 951 Lehman, R.M., Colwell, F.S., and Bala, G.A. (2001). Attached and unattached microbial
952 communities in a simulated basalt aquifer under fracture- and porous-flow conditions.
953 *Appl Environ Microbiol* 67, 2799-2809. doi: 10.1128/aem.67.6.2799-2809.2001.
- 954 Mann, A.J., Hahnke, R.L., Huang, S., Werner, J., Xing, P., Barbeyron, T., Huettel, B., Stuber,
955 K., Reinhardt, R., Harder, J., Glockner, F.O., Amann, R.I., and Teeling, H. (2013).
956 The genome of the alga-associated marine flavobacterium *Formosa agariphila* KMM
957 3901T reveals a broad potential for degradation of algal polysaccharides. *Appl*
958 *Environ Microbiol* 79, 6813-6822. doi: 10.1128/AEM.01937-13.
- 959 McBride, M.J. (2001). Bacterial Gliding Motility: Multiple Mechanisms for Cell Movement
960 over Surfaces. *Annual Review of Microbiology* 55, 49-75. doi:
961 10.1146/annurev.micro.55.1.49.
- 962 Morin, P.J. (2011). *Community Ecology*. Wiley.

- 963 Muth, T., Kolmeder, C.A., Salojärvi, J., Keskitalo, S., Varjosalo, M., Verdam, F.J., Rensen,
964 S.S., Reichl, U., de Vos, W.M., Rapp, E., and Martens, L. (2015). Navigating through
965 metaproteomics data: A logbook of database searching. *PROTEOMICS* 15, 3439-
966 3453. doi: 10.1002/pmic.201400560.
- 967 Nan, B., and Zusman, D.R. (2011). Uncovering the Mystery of Gliding Motility in the
968 Myxobacteria. *Annual Review of Genetics* 45, 21-39. doi: 10.1146/annurev-genet-
969 110410-132547.
- 970 Newton, R.J., Jones, S.E., Eiler, A., McMahon, K.D., and Bertilsson, S. (2011). A guide to
971 the natural history of freshwater lake bacteria. *Microbiology and Molecular Biology*
972 *Reviews* 75, 14-49.
- 973 Ng, C., DeMaere, M.Z., Williams, T.J., Lauro, F.M., Raftery, M., Gibson, J.A., Andrews-
974 Pfannkoch, C., Lewis, M., Hoffman, J.M., Thomas, T., and Cavicchioli, R. (2010).
975 Metaproteogenomic analysis of a dominant green sulfur bacterium from Ace Lake,
976 Antarctica. *ISME J* 4, 1002-1019. doi: 10.1038/ismej.2010.28.
- 977 Nobel, P.S. (2005). "5 - Photochemistry of Photosynthesis," in *Physicochemical and*
978 *Environmental Plant Physiology (Third Edition)*, ed. P.S. Nobel. (Burlington:
979 Academic Press), 219-266.
- 980 O'Neil, J.M., Davis, T.W., Burford, M.A., and Gobler, C.J. (2012). The rise of harmful
981 cyanobacteria blooms: The potential roles of eutrophication and climate change.
982 *Harmful Algae* 14, 313-334. doi: 10.1016/j.hal.2011.10.027.
- 983 Ogunseitan, O.A. (1993). Direct extraction of proteins from environmental samples. *Journal*
984 *of Microbiological Methods* 17, 273-281. doi: [http://dx.doi.org/10.1016/0167-](http://dx.doi.org/10.1016/0167-7012(93)90056-N)
985 [7012\(93\)90056-N](http://dx.doi.org/10.1016/0167-7012(93)90056-N).
- 986 Pandhal, J., Snijders, A.P., Wright, P.C., and Biggs, C.A. (2008). A cross-species quantitative
987 proteomic study of salt adaptation in a halotolerant environmental isolate using 15N
988 metabolic labelling. *Proteomics* 8, 2266-2284. doi: 10.1002/pmic.200700398.
- 989 Pérez, M.T., Rofner, C., and Sommaruga, R. (2015). Dissolved organic monomer partitioning
990 among bacterial groups in two oligotrophic lakes. *Environmental Microbiology*
991 *Reports* 7, 265-272. doi: 10.1111/1758-2229.12240.
- 992 Perkins, T.L., Clements, K., Baas, J.H., Jago, C.F., Jones, D.L., Malham, S.K., and
993 McDonald, J.E. (2014). Sediment Composition Influences Spatial Variation in the
994 Abundance of Human Pathogen Indicator Bacteria within an Estuarine Environment.
995 *PLoS ONE* 9, e112951. doi: 10.1371/journal.pone.0112951.
- 996 Schindler, D.W., Hecky, R.E., Findlay, D.L., Stainton, M.P., Parker, B.R., Paterson, M.J.,
997 Beaty, K.G., Lyng, M., and Kasian, S.E. (2008). Eutrophication of lakes cannot be
998 controlled by reducing nitrogen input: results of a 37-year whole-ecosystem
999 experiment. *Proc Natl Acad Sci U S A* 105, 11254-11258. doi:
1000 10.1073/pnas.0805108105.
- 1001 Schloss, P.D., Westcott, S.L., Ryabin, T., Hall, J.R., Hartmann, M., Hollister, E.B.,
1002 Lesniewski, R.A., Oakley, B.B., Parks, D.H., Robinson, C.J., Sahl, J.W., Stres, B.,
1003 Thallinger, G.G., Van Horn, D.J., and Weber, C.F. (2009). Introducing mothur: open-
1004 source, platform-independent, community-supported software for describing and
1005 comparing microbial communities. *Appl Environ Microbiol* 75, 7537-7541. doi:
1006 10.1128/aem.01541-09.
- 1007 Schweitzer, B., Huber, I., Amann, R., Ludwig, W., and Simon, M. (2001). Alpha- and beta-
1008 Proteobacteria control the consumption and release of amino acids on lake snow
1009 aggregates. *Appl Environ Microbiol* 67, 632-645. doi: 10.1128/AEM.67.2.632-
1010 645.2001.
- 1011 Sowell, S.M., Abraham, P.E., Shah, M., Verberkmoes, N.C., Smith, D.P., Barofsky, D.F., and
1012 Giovannoni, S.J. (2011a). Environmental proteomics of microbial plankton in a highly

1013 productive coastal upwelling system. *ISME J* 5, 856-865. doi:
1014 10.1038/ismej.2010.168.

1015 Sowell, S.M., Abraham, P.E., Shah, M., Verberkmoes, N.C., Smith, D.P., Barofsky, D.F., and
1016 Giovannoni, S.J. (2011b). Environmental proteomics of microbial plankton in a
1017 highly productive coastal upwelling system. *ISME J* 5, 856-865. doi:
1018 10.1038/ismej.2010.168.

1019 Sowell, S.M., Wilhelm, L.J., Norbeck, A.D., Lipton, M.S., Nicora, C.D., Barofsky, D.F.,
1020 Carlson, C.A., Smith, R.D., and Giovannoni, S.J. (2009). Transport functions
1021 dominate the SAR11 metaproteome at low-nutrient extremes in the Sargasso Sea.
1022 *ISME J* 3, 93-105. doi: 10.1038/ismej.2008.83.

1023 Teeling, H., Fuchs, B.M., Becher, D., Klockow, C., Gardebrecht, A., Bennke, C.M.,
1024 Kassabgy, M., Huang, S., Mann, A.J., Waldmann, J., Weber, M., Klindworth, A.,
1025 Otto, A., Lange, J., Bernhardt, J., Reinsch, C., Hecker, M., Peplies, J., Bockelmann,
1026 F.D., Callies, U., Gerds, G., Wichels, A., Wiltshire, K.H., Glockner, F.O., Schweder,
1027 T., and Amann, R. (2012). Substrate-controlled succession of marine bacterioplankton
1028 populations induced by a phytoplankton bloom. *Science* 336, 608-611. doi:
1029 10.1126/science.1218344.

1030 Teikari, J., Österholm, J., Kopf, M., Battchikova, N., Wahlsten, M., Aro, E.-M., Hess, W.R.,
1031 and Sivonen, K. (2015). Transcriptomics and proteomics profiling of *Anabaena* sp.
1032 Strain 90 under inorganic phosphorus stress. *Applied and Environmental*
1033 *Microbiology*. doi: 10.1128/aem.01062-15.

1034 Tilzer, M.M. (1987). Light-dependence of photosynthesis and growth in cyanobacteria:
1035 Implications for their dominance in eutrophic lakes. *New Zealand Journal of Marine*
1036 *and Freshwater Research* 21, 401-412. doi: 10.1080/00288330.1987.9516236.

1037 Van den Meersche, K., Middelburg, J.J., Soetaert, K., van Rijswijk, P., Boschker, H.T.S., and
1038 Heip, C.H.R. (2004). Carbon-nitrogen coupling and algal-bacterial interactions during
1039 an experimental bloom: Modeling a ¹³C tracer experiment. *Limnology and*
1040 *Oceanography* 49, 862-878. doi: 10.4319/lo.2004.49.3.0862.

1041 Wang, Y., and Spalding, M.H. (2014). Acclimation to very low CO₂: contribution of limiting
1042 CO₂ inducible proteins, LCIB and LCIA, to inorganic carbon uptake in
1043 *Chlamydomonas reinhardtii*. *Plant Physiol* 166, 2040-2050. doi:
1044 10.1104/pp.114.248294.

1045 Williams, T.J., and Cavicchioli, R. (2014). Marine metaproteomics: deciphering the
1046 microbial metabolic food web. *Trends Microbiol* 22, 248-260. doi:
1047 10.1016/j.tim.2014.03.004.

1048 Williams, T.J., Wilkins, D., Long, E., Evans, F., DeMaere, M.Z., Raftery, M.J., and
1049 Cavicchioli, R. (2013). The role of planktonic Flavobacteria in processing algal
1050 organic matter in coastal East Antarctica revealed using metagenomics and
1051 metaproteomics. *Environ Microbiol* 15, 1302-1317. doi: 10.1111/1462-2920.12017.

1052 Wood, A.M., and Van Valen, L.M. (1990). Paradox lost? On the release of energy-rich
1053 compounds by phytoplankton. *Marine Microbial Food Web* 4, 103-116.

1054 Yeates, T.O., Kerfeld, C.A., Heinhorst, S., Cannon, G.C., and Shively, J.M. (2008). Protein-
1055 based organelles in bacteria: carboxysomes and related microcompartments. *Nat Rev*
1056 *Microbiol* 6, 681-691. doi: 10.1038/nrmicro1913.

1057 Yutin, N., Suzuki, M.T., Teeling, H., Weber, M., Venter, J.C., Rusch, D.B., and Beja, O.
1058 (2007). Assessing diversity and biogeography of aerobic anoxygenic phototrophic
1059 bacteria in surface waters of the Atlantic and Pacific Oceans using the Global Ocean
1060 Sampling expedition metagenomes. *Environ Microbiol* 9, 1464-1475. doi:
1061 10.1111/j.1462-2920.2007.01265.x.

1062 Zhang, J., Kobert, K., Flouri, T., and Stamatakis, A. (2014). PEAR: a fast and accurate
1063 Illumina Paired-End reAd mergeR. *Bioinformatics* 30, 614-620. doi:
1064 10.1093/bioinformatics/btt593.
1065
1066

Provisional

Figure 01.JPEG

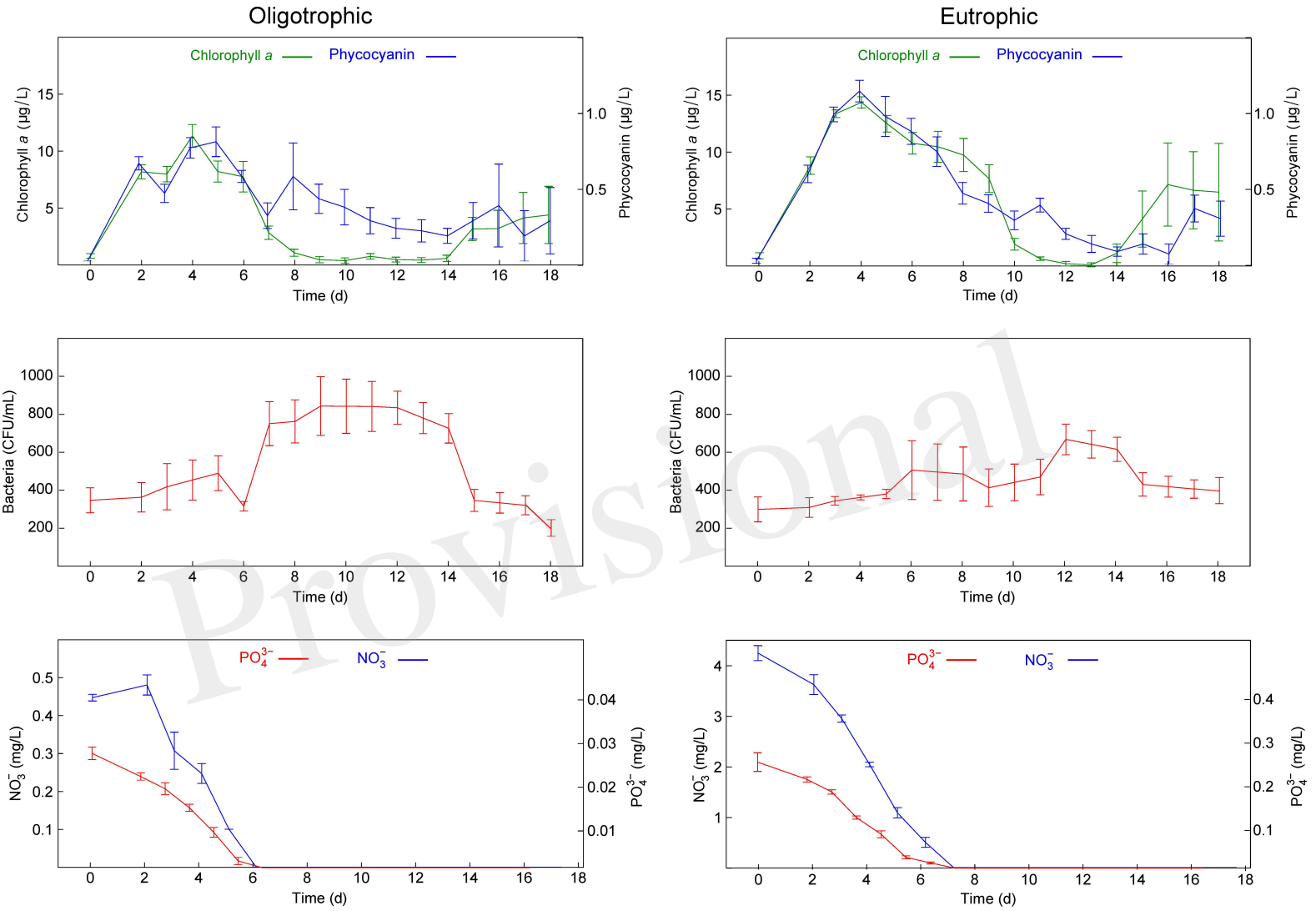


Figure 02.JPEG

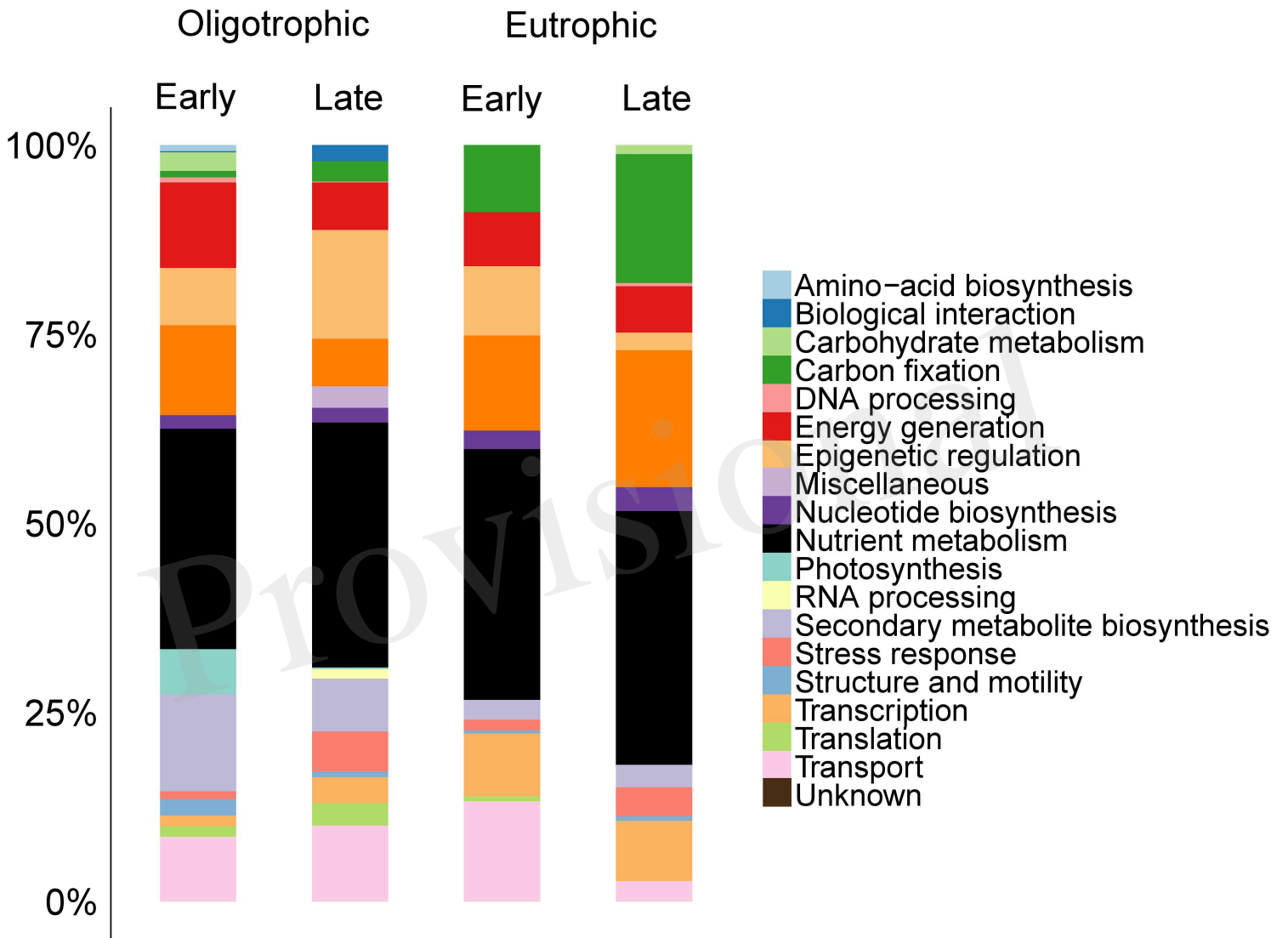


Figure 03.JPEG

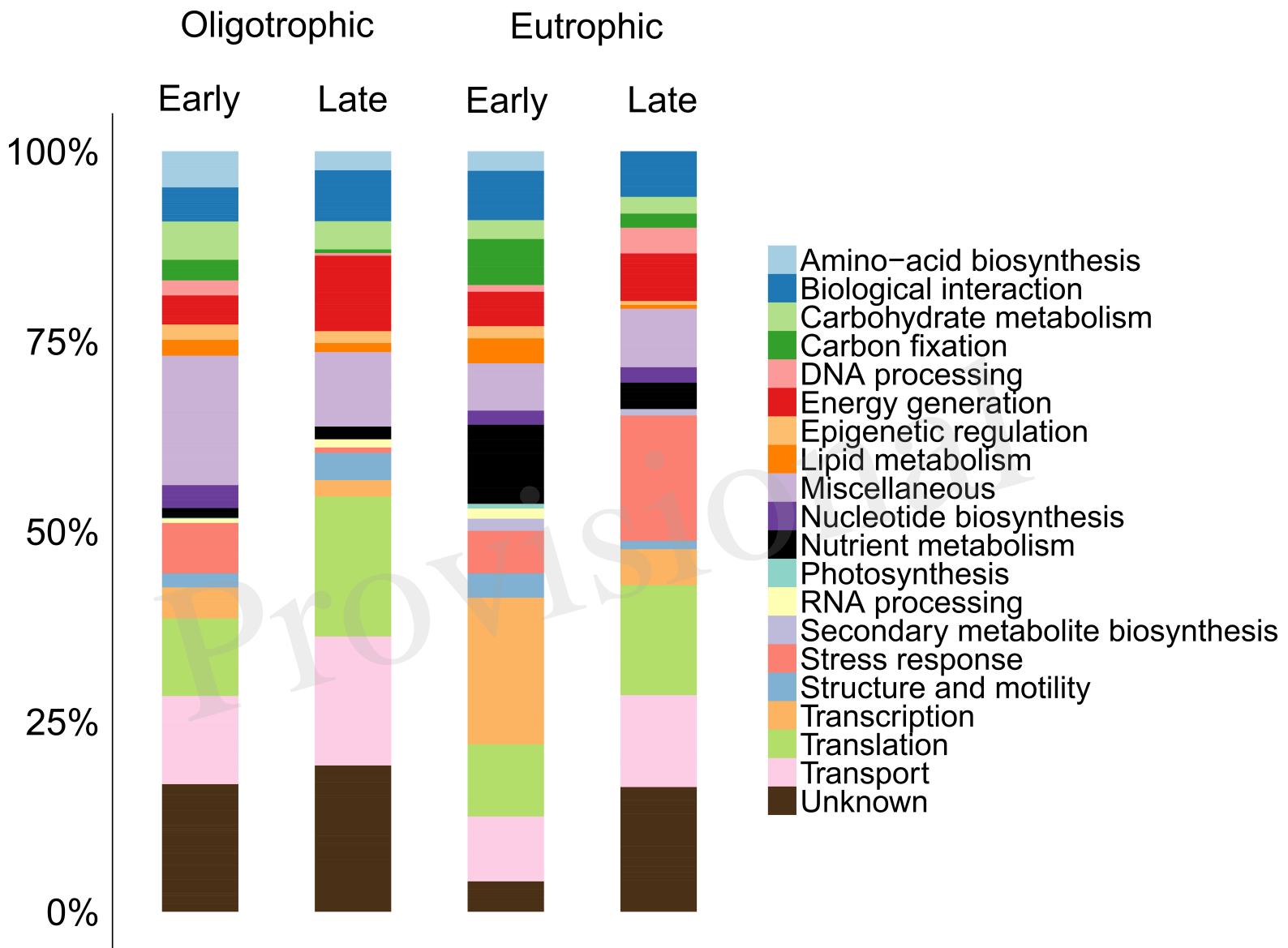


Figure 04.JPEG

